Rapidly solidified nickel-base superalloys

J. V. WOOD
Faculty of Technology, The Open University, Walton Hall, Milton Keynes, UK

P. F. MILLS, A. R. WAUGH, J. V. BEE[*]
Department of Metallurgy and Materials Science, University of Cambridge, Cambridge, UK

The structures of rapidly solidified APK1, In 100 and low-carbon In 792 are described and compared with that of Nimonic 80A. Under identical processing conditions, cellular, dendritic and homogeneous equiaxed structures can be obtained. This is not due to either the influence of cooling conditions or to any single alloying addition, but depends on the combined effects of the Ti, Cr and C contents. The spinodal-type formation of γ', proposed for Nimonic 80A, cannot be suppressed in these alloys by pendant drop melt extraction or melt spinning techniques. However, detailed atom-probe field-ion microscopy suggests that the γ' formation in APK1 does develop by a similar mechanism. Although not directly attributable to a modulated microstructure or to the presence of disordered particles, the extremely high strength levels observed in this alloy after heat treatment are due to the subsequent development of small, ordered, γ' precipitates in a fine-grained matrix, together with the absence of deleterious grain boundary carbide precipitation.

1. Introduction

The development of powder production routes for nickel-base alloys used in gas turbine engines, for example [1], has generated widespread interest in the selection of optimum alloy compositions which will maximize the benefits obtainable by these techniques. During the last decade, improvements in gas atomization processes have led to an increase in the quench rate to between 10^4 and 10^6 K sec^{-1}. A recent report [2] indicated that substantial improvements in some high temperature properties can be achieved in consolidated components made by this route.

While it is not possible to summarize in this paper the general advantages of this production route, those effects which are relevant to the rapid solidification of nickel-base superalloys are listed.

(a) Small initial grain size values between 0.1 and 10 μm can be obtained depending on the exact alloy composition and the specific pro-

cessing method. This is normally achieved by the large undercoolings that occur in most liquid quenching techniques (of the order of 200 K) which can promote homogeneous nucleation.

(b) Reduction or elimination of solute segregation. The large undercoolings which are maintained during most of the solidification reaction enable the liquid–solid interface to move at a relatively high velocity (~ 0.1 m sec^{-1}). Thus the secondary dendrite arm spacing is often less than 0.25 μm and, in the extreme, segregation can totally be suppressed, (the grains grow by a planar interface movement).

(c) Large increases in "quenched in" vacancy concentrations can occur in f c c metals [3]. These either collapse to form dislocation loops, which subsequently act as precipitate nucleation sites, or associate with solute atoms and modify the nature of the precipitating phase [4].

(d) Increases in the terminal solid solubility of alloying additions (for example, Ti, Al, C) can be

---

[*]Present address; Department of Metallurgy, University of Witwatersurand, Johannesburg, South Africa.

obtained. This could provide higher volume fractions of the principal strengthening component γ': ordered Ni_3 (Al, Ti).

(e) Precipitation reactions may be modified, resulting in either different structures or morphologies of second phase particles.

Since rapidly solidified superalloys are unlikely to find significant use in the "as-quenched" form (apart from laser glazed components) there are three distinct difficulties which must be considered when further consolidation and heat treatment schedules are required:

(a) The large grain boundary area can act as a preferred nucleation site for continuous precipitate films which give rise to very low tensile strengths [5];

(b) The large surface area inherent in rapidly solidified products (particularly powders) promotes segregation of certain elements (carbon, oxygen and sulphur [6]) to the free surface, which markedly affects the consolidation parameters;

(c) It is difficult to induce grain growth, since the uniform distribution of grain size and the generally low dislocation density of the materials provide little driving force for recrystallization.

However, it is possible to minimize these difficulties. Deleterious carbide precipitation on grain boundaries and particle surfaces can be avoided by either the removal of carbon from the alloy or by the addition of a surface active component, such as boron. In order to achieve recrystallization, materials can be subjected to thermo-mechanical processing.

Our initial experiments concentrated on a high carbon, low aluminium and titanium alloy: Nimonic 80A [7]. During heat treatment at 760° C, $M_{23}C_6$ formed after very short ageing times (5 minutes), either as a continuous film on the grain boundaries or, associated with ordered γ', via a discontinuous reaction. At the same time, an unconventional matrix precipitation sequence was observed. Initially, a disordered phase Ni_3 (Al, Ti, Cr), developed by a spinodal-type reaction. On further ageing, the structure became that of ordered γ', Ni_3 (Al, Ti), as chromium diffused out of the precipitate.

The fracture surfaces of these aged specimens showed intergranular failure by crack propagation along the embrittled grain boundaries [8]. It was not therefore possible to determine the effect of the metastable disordered precipitate on the tensile strength.

The present paper concentrates on work conducted on a low carbon alloy (0.03 wt% C), APK1, which has been developed by Henry Wiggin and Co. Ltd., Hereford, for argon gas atomization. The major constituents are listed in Table I, together with the compositions of other commercial alloys considered in this paper. In addition to having a lower carbon level than Nimonic 80A, APK1 has a higher concentration of aluminium and titanium (γ'-forming elements) and was therefore thought to be a more suitable alloy for the determination of the effect of such a spinodal reaction on mechanical properties.

2. Experimental procedure

Samples of the alloy were provided in the form of 10 mm diameter extruded rods suitable for processing by either pendant drop melt extraction (PDME) or melt spinning [9]. These processes were performed in a vacuum chamber which was evacuated to 10^{-2} Pa after it had been flushed twice with helium. The chamber was then backfilled with helium before melting. 0.15 m diameter copper wheels were used with a peripheral speed of about $10\,\text{m\,sec}^{-1}$. Using the PDME technique, fine wires ($\sim 50\,\mu\text{m}$ diameter) were drawn by a sharp edged wheel from a molten drop on the end of a rod. For melt spinning, small buttons of molten alloy were ejected onto a flat wheel through a 1 mm orifice in a quartz crucible. Heat was generated by an r.f. induction coil. There was no visible contamination of either the resultant wire or the

T A B L E I Analysis of nickel superalloys in weight per cent (major elements only)

	C	Ti	Al	Mo	Cr	Co	Ni
Nimonic 80A	0.10	2.7	1.6	–	21	2.0	balance
APK1	0.03	3.6	4.1	5.2	16	15	balance
In 100	0.18	4.7	5.5	3.0	10	15	balance
In 972 (low-carbon)	0.10	4.2	3.2	2.0	13	19	balance

ribbon after quenching, and no subsequent evidence suggested any gas pickup. The effect of gas atmospheres had been discussed previously [5]. The wires were suitable for the field-ion atom-probe microscopes after thinning to give a small radius tip. Ribbons were thinned for transmission electron microscope using conventional techniques, and examined in a Philips EM 301.

Two types of atom-probe field-ion microscopes were used in this project. In these instruments atoms on the specimen surface are ionized (field-evaporated) by an intense electric field and subsequently mass-analysed by a time-of-flight spectrometer. In one instrument, the spectrometer accepts ions which have originated from a very small area of the surface, of about 1 to 2 nm in diameter, and consequently the progressive removal of the surface layers by ionization allows a narrow cylinder of material to be sampled, so that a composition profile can be plotted along the specimen length with resolution of about 1 nm. In the second instrument, ions from a larger area, of about 30 to 35 nm, are accepted and an image-forming spectrometer is used to produce elemental maps which show the place of origin of the various ionic species. The individual ionic resolution is again between 1 and 2 nm, but if particles protrude from the field ion tip this can lead to differences in local magnification which must be taken into account when analysing the ionic distribution. The techniques and errors involved are described elsewhere [10, 11].

Room temperature tensile tests were performed on a special cradle attached to a low load servo-controlled machine. The cross-sectional area was measured after the test using a scanning electron microscope.

3. Results
3.1. The as-solidified alloys
3.1.1. As-solidified APK1
The solidification structures of both wire and ribbon show no evidence of dendritic growth, and all grains throughout the cross-section appear equiaxed (Fig. 1). This is unexpected since APK1 in the as-received powder form (produced by argon atomization) is dendritic with a secondary dendrite arm spacing of about 2 μm [1]. Dendrites are also found occasionally in melt extracted Nimonic 80A but in this case the secondary dendrite arm spacing is only about 0.5 μm. In such a complex alloy as APK1 the effects of various

alloying elements on the freezing range are not readily available. However for homogeneous nucleation to occur, thus giving the observed fine equiaxed grains of 1 to 5 μm diameter, contact with the wheel must lead to sufficient undercooling below the solidus to prevent dendritic growth.

The internal grain structures revealed by transmission electron microscopy confirms the lack of regular dendrite arms although a number of low angle boundaries (Fig. 2a) are found within grains. These are not obviously associated with the solidification structure, since they are randomly distributed throughout the grains. Occasionally, carbides are observed within the matrix (Fig. 2b) and these have been analysed using the atom-probe microscope. The analysis from one such particle (shown in Fig. 3) gives the approximate composition: (Ti, Cr) (C, N). This precipitate is less deficient in carbon and nitrogen than similar particles found in Nimonic 80A, which were found to have a typical carbonitride defect structure. However as there is a wide variation in the deviation from the stoichiometric MX composition found in rapidly solidified alloys [12], it would require analysis of a large number of particles to prove that there is any significant difference between APK1 and Nimonic 80A. The population of these carbides in the matrix is small, and such an analysis is unrealistic for a technique such as atom-probe microscopy. By using identical polishing conditions to those used for Nimonic 80A and several other nickel alloys, a thin foil which did not contain the background mottled effect shown in Fig. 2b could not be obtained. Thus, in this alloy, it is not possible to suppress the spinodal decomposition reaction by rapid solidification. However, superlattice reflections were not observed in the diffraction patterns from any of the specimens, and it is concluded that the observed structures represent the early stages of γ' formation.

The element imaging patterns from as-quenched APK1 are shown in Fig. 4a. An inhomogeneous distribution of all the elements is observed, and is most clearly visible as banding in the nickel and chromium images. Although the partitioning of titanium and aluminium is less evident, this is due to the effect of surface topography on the local magnification for these species [11]. It is estimated that the elliptical areas of low chromium concentration are about 10 nm long by 5 nm or less wide, although there is no distinct edge.
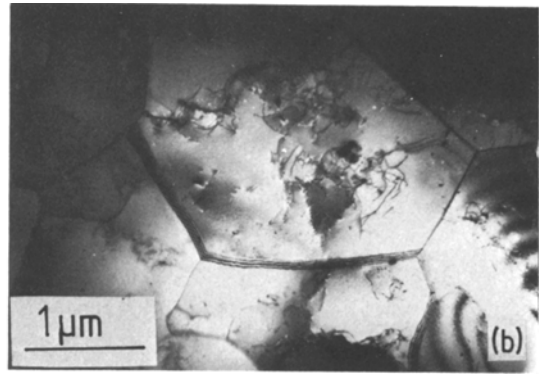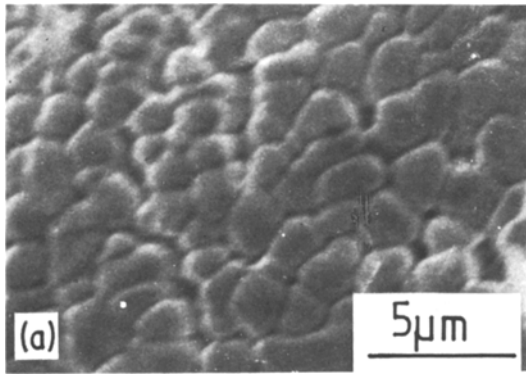
Figure 1 (a) Scanning electron micrograph of PDME wire of APK1; (b) transmission electron micrograph of melt spun APK1 ribbon.

Fig. 5a shows examples of typical traces for each element as the field-ion tips were sectioned by field evaporation, and the ionic species monitored. Four deductions can be made from these data:

(a) In the direction of this analysis, the aluminium- and titanium-rich particles are spaced between 10 and 20 nm;

(b) The chromium concentration rises to a maximum of 20 at % in the matrix, but only falls to about 7 at % within the particles;

(c) There is some evidence that molybdenum partitions with the chromium;

(d) The combined (Ti + Al) concentration is already at the level of 25 at % necessary for γ' formation.

For comparison, the structures determined by transmission electron microscopy from a preliminary study of two other rapidly solidified superalloys with high Ti and Al contents are also reported: In 100 and low-carbon In 792, (see Table I).

3.1.2. As-solidified In 100

This alloy has a significantly higher carbon level than APK1 (0.18 wt% max.) and also contains approximately 1 wt % more of both Al and Ti. The structure of the as-quenched sample is shown in Fig. 6. The grain size is of the order of 2 to 5 μm and, as in APK1, there is evidence of low angle boundary formation (Fig. 6a). In the larger grains a more regular array of low angle boundaries is observed although the structures never become cellular. However in the "as-quenched" conditions carbide particles are found both within the grains and at the grain boundaries indicating that the quench rate has not been sufficient to suppress carbide formation. The diffraction patterns from
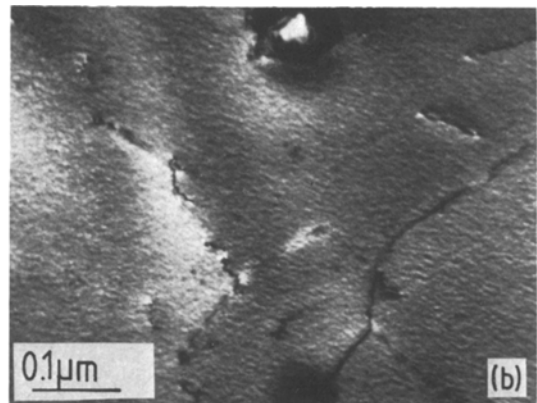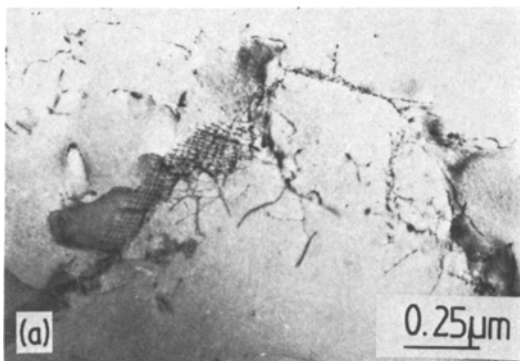

Figure 2 Transmission electron micrographs of "as-quenched" APK1: (a) low-angle boundary formation; (b) mottled matrix and undissolved carbide.
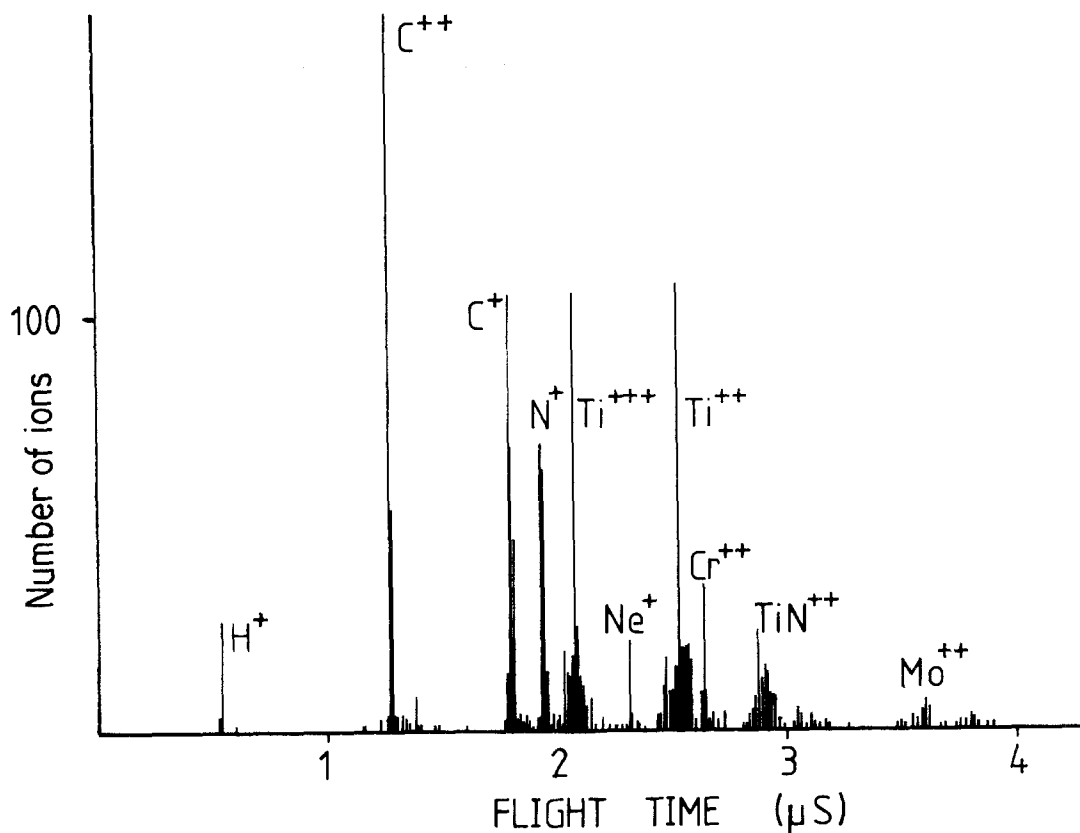
2712

Figure 3 Atom-probe spectrum from carbide particle similar to that shown in Fig. 2b.

all areas indicate the presence of ordered γ' in the matrix (Fig. 6b). The particle size appears to vary between 10 nm and 20 nm.

3.1.3. As-solidified low-carbon In 792

This modified composition has a carbon-level intermediate between In 100 and APK1. The total concentration of Ti and Al is similar to APK1, although the ratio of Al:Ti is reversed. Again there is some evidence of grain boundary carbide precipitation (Fig. 7a) and also a fine matrix precipitate which gives rise to super-lattice reflections from the larger grains (Fig. 7b). It would appear that this alloy represents an inter-mediate state between APK1 and In 100 with respect to the appearance of matrix γ' precipitates. Thus it is suggested that there is a maximum con-centration of Ti and Al which can be retained in solution by rapid solidification from the melt. That level is necessarily determined in each alloy by the relative activities of the remaining alloying

elements present, but it would appear to be of the order of 3.5 wt % Ti and 4.0 wt % Al.

3.2. Heat treated structures in APK1

The heat treatment temperature was chosen as $760°$ C since this represents the final stage of the conventional heat treatment schedule for APK1. Conveniently, this also corresponds to the heat treatment originally applied to rapidly solidified Nimonic 80A [5].

Fig. 8 shows well-developed ordered γ' pre-cipitates observed after 2.7×10^3 sec at $760°$ C. The data from atom-probe microscopy for various heat treatment times are reproduced in Figs. 4 and 5. The partitioning of elements is clearly evident after 1.2×10^3 sec (Figs. 4b and 5b). At this stage of development, the particles contain 3 at % or less chromium and there is evidence from individual spectra that both cobalt and molybdenum diffuse sympathetically with chromium. The distinct particles seen in all the elemental images after
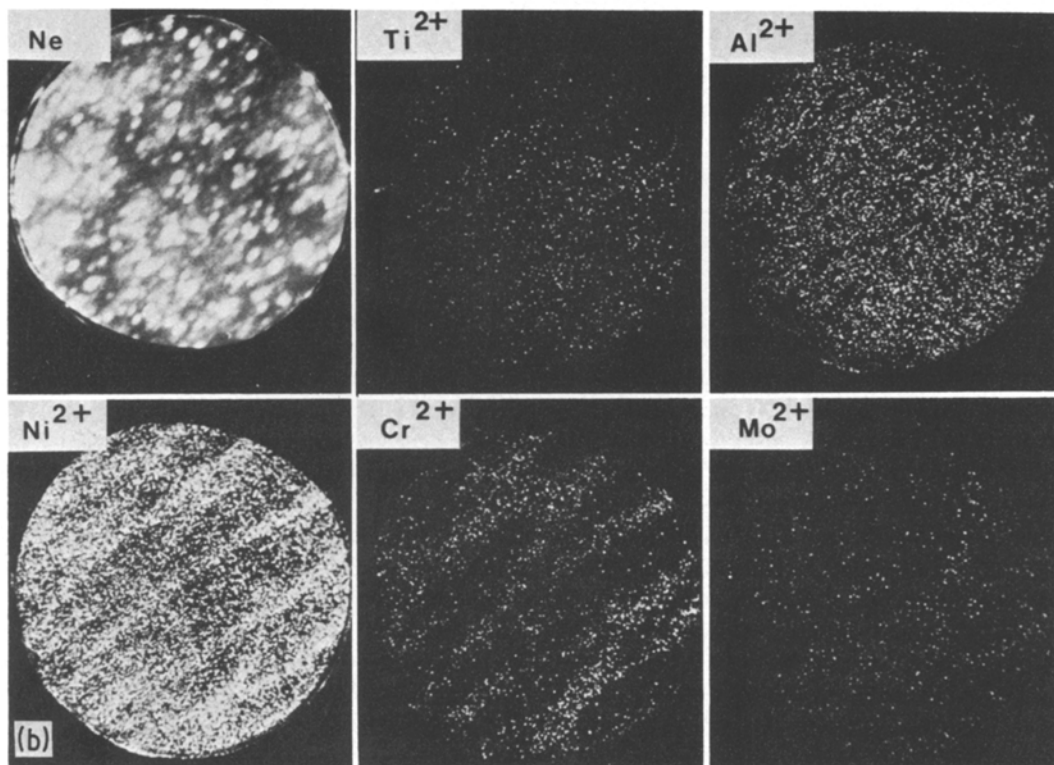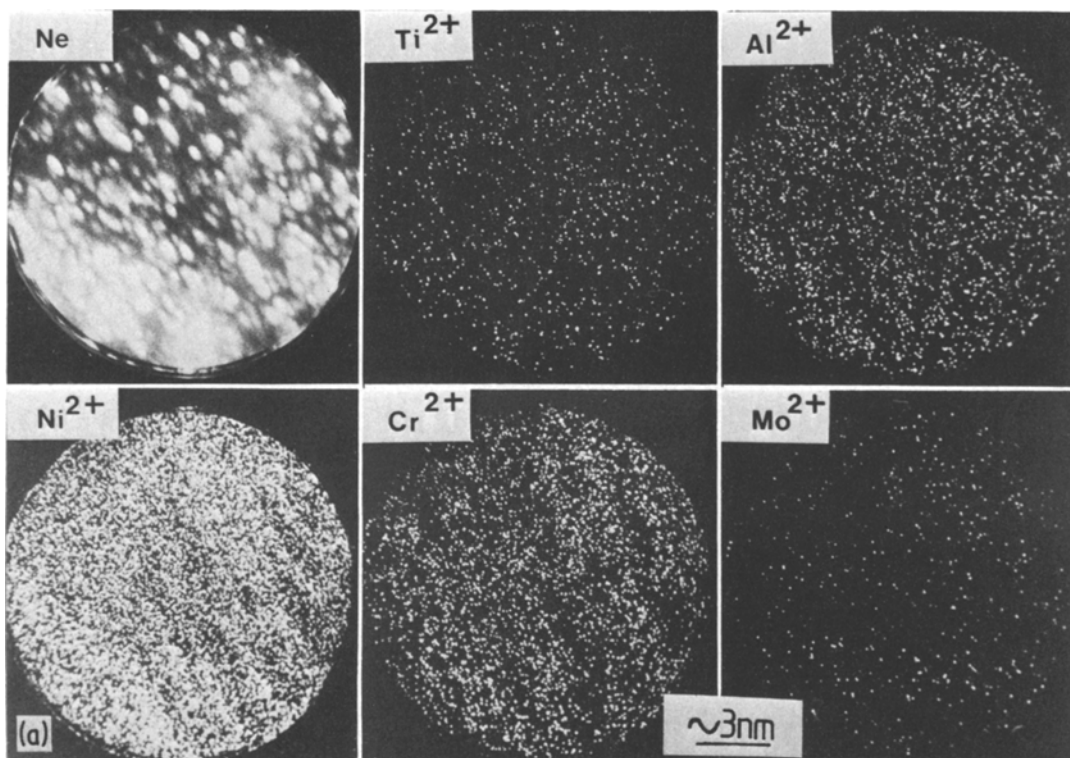
Figure 4 Atom-probe elemental imaging patterns in APK1: (a) as-quenched; (b) heat treatment for 1.2×10^3 sec at 760° C; (c) heat treatment for 9×10^3 sec at 760° C.
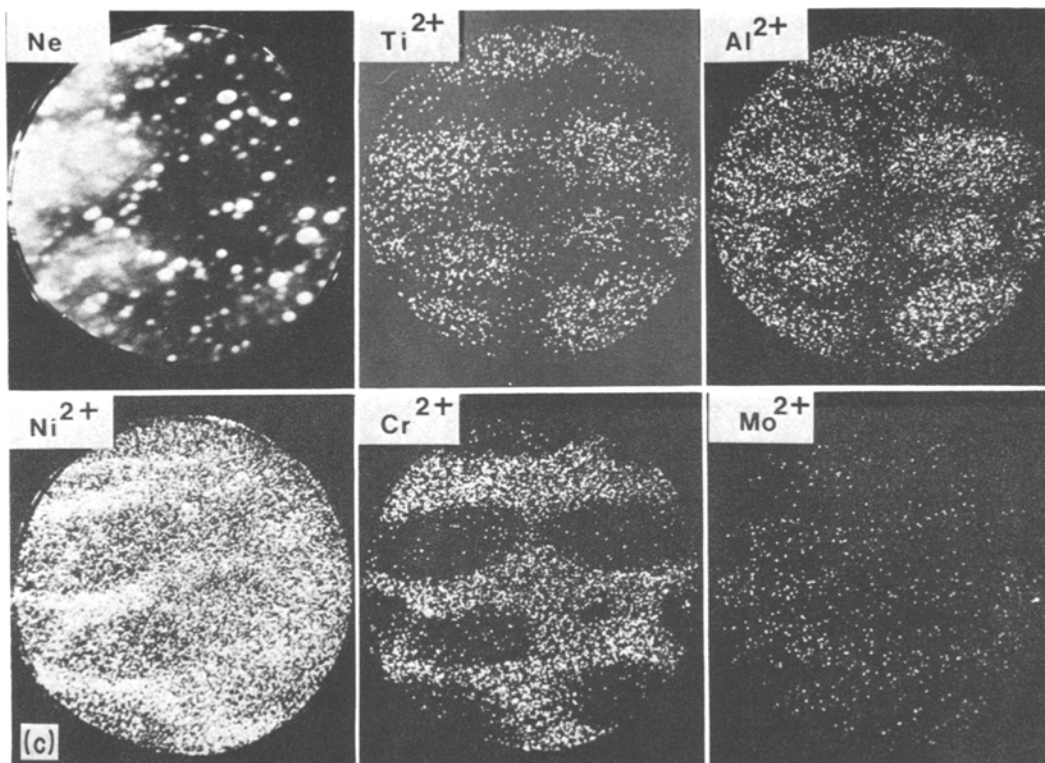
Figure 4 Continued.

9×10^3 sec at 760° C (Figs. 4c and 5c) correspond to the ordered precipitates observed by transmission electron microscopy (Fig. 8).

3.3. Mechanical properties of APK1

It is not proposed to present these data in detail as they have already been reported elsewhere [8]. The as-quenched tensile strength of rapidly solidified APK1 is of the order of 1200 MPa and exhibits a ductile failure mechanism at room temperature. After heat treatment the ultimate tensile strength exceeds 2000 MPa and values up to 4000 MPa have been measured, although there is a large degree of error in measuring the cross-sectional area in such specimens. However it is believed that very high strengths can be induced in this alloy after heat treatment.

4. Discussion.

The results of this investigation suggest that the microstructures of rapidly solidified superalloys are the result of the complex interaction of several variables, none of which individually display significant trends. This is clearly illustrated

in the case of carbon concentration, for which there is no obvious correlation between carbon content and solidification structure. In both APK1 (0.03 wt % C) and In 100 (0.18 wt % C), there is evidence of low angle boundary formation but no tendency to develop regular cells or dendrites. By contrast, at intermediate carbon levels in In 792 (0.1 wt % C) and Nimonic 80A (0.1 wt % C) processing under identical conditions gives rise to cellular and dendritic structures respectively.

Similarly the range of solidification structures cannot be explained solely in terms of the chromium content, which increases in the order In 100 (10 wt %), In 792 (13 wt %), APK1 (16 wt %) and Nimonic 80A (21 wt %).

It is also unlikely that the variation in the structures of these alloys is determined by a change in cooling conditions. The freezing range for Nimonic 80A is approximately 45 K and according to the Ni–Cr binary phase diagram [13] a reduction of Cr to between 10 and 15% would only reduce this by about 10 K. It is probable, therefore, that the freezing range does not change significantly between these alloys. Although it is
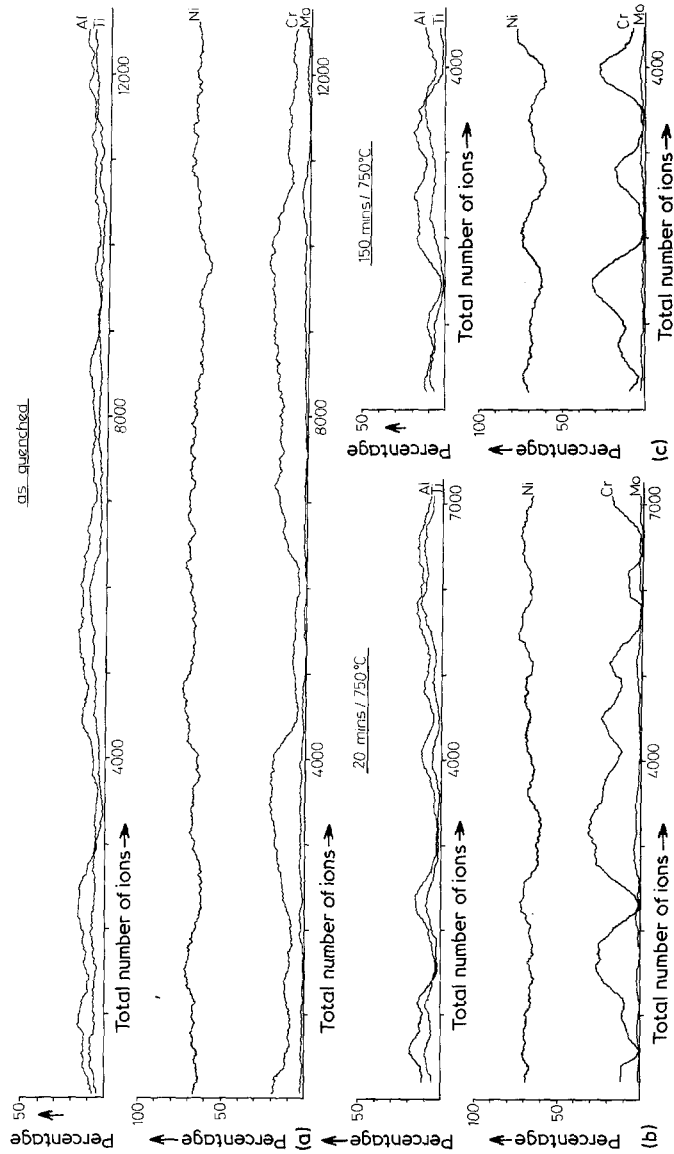
Figure 5 Atom-probe constitutional analyses along PDME fibres of APK1: (a) as-quenched; (b) heat treatment for 1.2×10^3 sec at $760°$ C. (c) heat treatment for 9×10^3 sec at $760°$ C. Scale: 1000 ions $\simeq$ 4 nm.
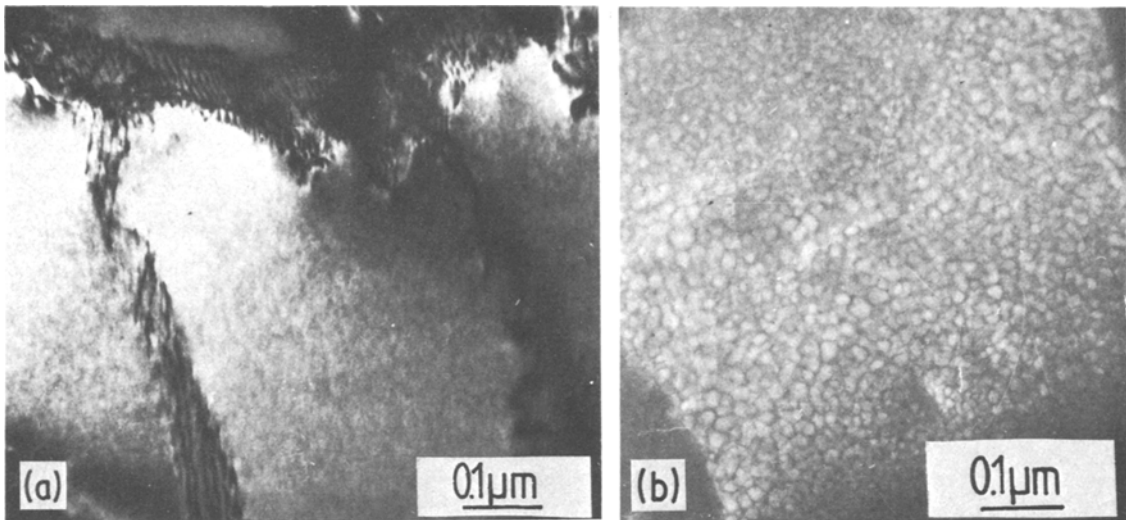
Figure 6 Melt spun In 100 (transmission electron micrographs): (a) low-angle boundary formation; (b) fine matrix γ' (dark field).

not possible within the given experimental conditions to determine the melt superheat, there is unlikely to be any significant difference in the quenching conditions for each alloy. It is generally accepted that a high degree of supercooling occurs during rapid solidification from the melt, and for the case of iron-base alloys this has been predicted as about 200 K [14]. In addition, in PDME, superheat has relatively little effect on the cooling profile [15]. It is probable therefore that the variation in structure between these alloys is in some way associated with the alloy composition.

In the case of PDME Nimonic 80A, TiC carbides can occasionally be found in the interdendritic spaces. Similar structures have been observed in rapidly solidified Fe–Ni–Cr steels containing relatively large carbon concentrations [12], except

that the particles in this case were $M_{23}C_6$ carbides. Although both types of carbides have a parallel orientation relationship with the matrix, they can align themselves during the solidification reaction [16] and are not necessarily formed during the solid state quenching regime. The nucleation of such particles ahead of the solidifying interface could then act as perturbation points for dendrite formation.

These results suggest that, for a given quench rate, it is necessary to have a critical activity of Cr, Ti and C in order to nucleate $M_{23}C_6$ or TiC in the melt prior to solidification of the matrix. This hypothesis is supported by observations in Ni–Cr austenitic steel, where, despite the close relationship in lattice parameter between $M_{23}C_6$ and γ, it is known that $M_{23}C_6$ and also TiC do not
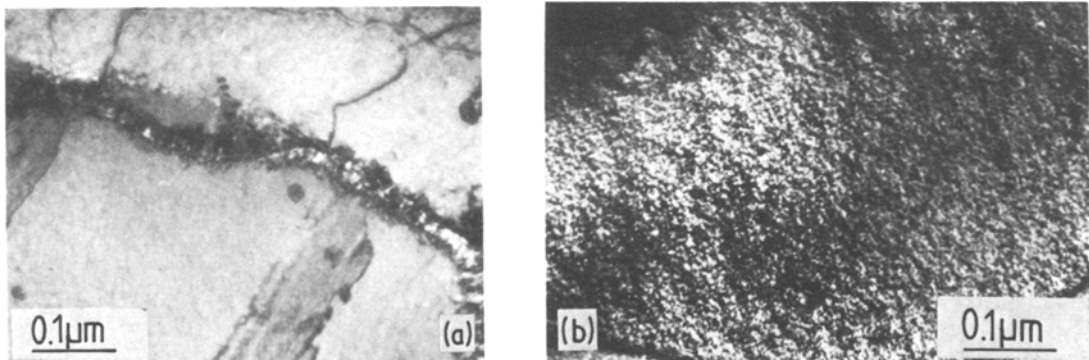

Figure 7 Melt spun In 792 (transmission electron micrographs): (a) $M_{23}C_6$ grain boundary precipitates; (b) fine γ' matrix precipitation.
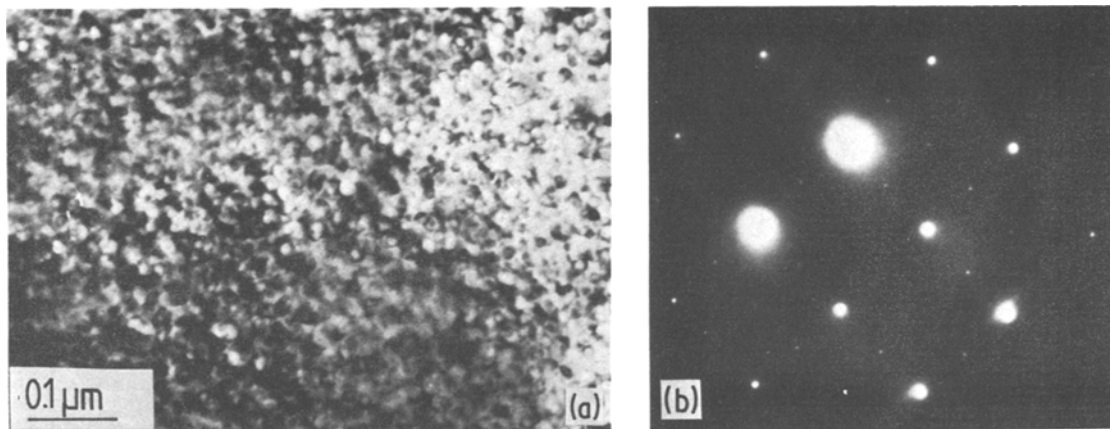
Figure 8 (a) γ' particles in APK1, aged at 760° C for 2.7 × 10³ sec; (b) diffraction pattern for the same area showing γ' superlattice reflections.

act as nucleating agents under normal casting conditions [17].

Powders of In 100 (about 100 μm in diameter), produced by high gas velocity atomization, have been shown to have a totally dendritic structure [18]. The secondary dendrite arm spacing varied between 0.5 and 1.0 μm, which corresponds to an approximate cooling rate of between 10⁴ and 10⁵ K sec⁻¹. The particles in the interdendritic regions were identified as (Mo, Ti) C type particles. It can therefore be assumed that PDME quenching gives a higher quench rate than that achieved in these large particles. However it has been reported [19] that there is a change to non-dendritic structures within rapidly solidified nickel superalloy powders of similar compositions below a critical particle size (normally less than 50 μm in diameter). It is suspected that a similar change should also occur in In 100 at a critical quench rate and that such a structure would be analogous to those reported in this paper.

In addition to the effect of alloy composition on the solidification structures of these alloys it was hoped that more could be discovered about the possible spinodal reaction which has already been identified in rapidly solidified Nimonic 80A [7]. Clearly in the case of both In 100 and In 792 this pre-precipitation reaction cannot be suppressed by these particular rapid solidification techniques. In APK1, although rapid solidification does not prevent the formation of particles, analyses have shown that these still contain about 7 at % Cr. This suggests that they probably correspond to the disordered Ni_3 (Al, Ti, Cr) particles previously observed in Nimonic 80A [7]. During heat treat-

ment at 760° C, these original particles coarsen and reduce their interfacial energy, by progressing to a spherical morphology. After 1.2 × 10³ secs, the chromium content within the precipitates has already fallen to < 3 at %, and after 2.7 × 10³ sec they can be unambiguously identified as ordered γ'. These observations are consistent with the hypothesis already proposed for the initial formation of γ' by a spinodal type reaction, with the ordering of the precipitate delayed until sufficient chromium diffusion out of the precipitate has occurred [7].

The high strength levels observed in APK1 after heat treatment at 760° C is not therefore directly attributable to a spinodal type of structure nor to the presence of small disordered particles. However, this precipitation mechanism does provide the dense distribution of fine, ordered, γ' precipitates which have a potent strengthening effect.

5. Conclusions

(a) Both PDME and melt spinning techniques can be used to produce nickel superalloys with a homogeneous, fine-grained structure.

(b) At Ti and Al levels in excess of 3.5 wt % and 4 wt % respectively, these elements cannot be prevented from partitioning during the quench.

(c) APK1 is near this critical composition, but benefits from the lack of grain boundary carbide phases.

(d) The solidification structure of a rapidly quenched nickel based superalloy is dependent on the carbon, chromium and titanium concentrations, for a given quench rate.

(e) Very high strengths are obtainable in rapidly

solidified APK1 which are dependent on the fine grain size and the dispersion of small γ' particles.

Acknowledgements

References

1. L. WILLIAMS, *Powder Metallurgy* 2 (1977) 84.
2. D. J. LOOFT and E. C. VAN REUTH, Proceedings of the Conference on Rapid Solidification Processing, Reston Va., 1977 (Claitor Publishing, Baton Rouge, 1978) p. 1.
3. G. THOMAS and R. M. WILLENS, *Acta Met.* 14 (1966) 1385.
4. S. C. AGARWA and H. HERMAN, Proceedings of the Conference on Phase Transitions (Pergamon Press, Oxford, 1973) p. 207.
5. J. V. WOOD, J. K. BINGHAM and J. V. BEE, Proceedings of the 3rd International Conference on Rapidly Solidified Alloys, (Metals Society 1978), p. 94.
6. P. N. ROSS and B. H. KEAR, Proceedings of the 3rd International Conference on Rapidly Solidified Alloys, Brighton (Metals Society, 1979) p. 102.
7. J. V. WOOD, P. F. MILLS, J. K. BINGHAM and J. V. BEE, *Met. Trans.* 10A (1979) 575.
8. J. V. WOOD and J. V. BEE, Proceedings of the 5th International Conference on the strength of metals and alloys, Aachen, 1979 (Pergamon, Oxford, 1979) p. 711.
9. R. B. POND, R. E. MARINGER and C. E. MOBLEY, "New Trends in Materials Processing" (ASTM, 1974) p. 128.
10. M. J. SOUTHON, E. D. BOYES, P. J. TURNER and A. R. WAUGH, *Surface Sci.* 53 (1975) 554.
11. A. R. WAUGH and M. J. SOUTHON, *ibid.* 89 (1979) 718.
12. J. V. WOOD and R. W. K. HONEYCOMBE, *Phil. Mag.* 37A (1978) 501.
13. J. V. WOOD and K. AKHURST, *J. Mater. Sci.* 11 (1976) 2142.
14. S. R. ROBERTSON, T. J. GORUSCH and R. P. I. ADLER, Proceedings of the Conference on Rapid Solidification Processing, Reston Va., 1977 (Claitor Publishing, Baton Rouge, 1978) p. 188.
15. J. V. WOOD, "Solidification and Casting of Metals" (Metals Society, Sheffield, 1979) p. 179.
16. W. BETTERIDGE and J. HESLOP, Eds., "The Nimonic Alloys" (Edward Arnold, London, 1974) Ch. 4.
17. F. A. SHUNK, "Constitution of Binary Phase Diagrams" (McGraw-Hill, New York, 1969) p. 247.
18. R. C. RUHL, *Mater. Sci. Eng.* 1 (1967) 313.
19. D. H. WARRINGTON, University of Sheffield, private communication (1980).